Zero Bias H_∞ Control of Flexible Rotor Magnetic Bearing Flywheel System with Gyroscopic Effect Using Singular Value Decomposition

Ming Ren , Kenzo Nonami
Graduate School of Science and Technology
Chiba University 1-33,Yayoi-Cho,Inage-ku,Chiba-shi,
Chiba,263-8522 Japan nonami@faculty.chiba-u.jp

Atsushi Kubo, Hironori Kameno
Research & Development Center, JTEKT Corporation
No.333, Toichi-cho, Kashihara-shi, Nara 634-8555,
japan atsushi_kubo@jtekt.co.jp

Abstract – This investigation deals with a small flywheel energy storage rotor supported by magnetic bearing system. A flexible model based on finite-element method is derived. Thereafter, we proposed making a mode separation using singular value decomposition method when the gyroscopic matrix is considered in the equation of motion. Further, the reliability of reduced–order FEM model is verified and the five H∞controllers are designed to guarantee the whole stability up to 200Hz. The effectiveness of the reduced-order flexible model and the stability of the closed-loop system are verified by simulations.

Index Terms – Magnetic Bearing System, Gyroscopic Effect, Singular Value Decomposition, H∞ Control, Mode Separation, Vibration analysis,

I. INTRODUCTION

Most researches about magnetic bearing system have been presented based on rigid rotor which is usually considered as a concentration mass. However, in practice, numberless vibration modes exist in the rotor which has a distribution mass. They will bring the serious influence to stability of system. Meanwhile, the magnetic bearing with a large flywheel has a strong gyroscopic effect which makes the frequency of synchronous vibration of first bending backward mode low and approaches the synchronous vibration of the second rigid forward mode rapidly. So even if the controller of the rigid rotor considering the gyroscopic effect can be obtained, it is still difficult to make rotor rotate as a high speed for the above reasons.[1]

This paper takes into account of the gyroscopic effect of the flexible rotor. It is difficult to derive a flexible model directly from an equation of motion. Here, we can obtain the model using a numerical analysis of finite-element method (FEM). Nevertheless, the order of derived FEM model is too high to be used in control system design. Therefore, a reduced-order model is derived following the principles of L.Meirovith[2] about the mode separation technique considering gyroscopic effect. The cholsky decomposition is also used in this reference. However, the matrix is a semi-positive definite which can not satisfy the condition of Cholsky decomposition when the rotor is in the "free-free" condition. This paper proposes the singular value decomposition method instead of Cholsky decomposition method to acquire a reduced-order model which only includes four rigid modes and the first bending backward mode.

According to the characteristics that the natural frequencies of bending mode will keep its invariant, namely, the bending modes do not depend on the controller. So we did a vibration analysis based on rigid model using a controller which can make the system stable to obtain the relation between the natural frequency and the rotational frequency. So the FEM model can be adjusted similar to actual system Finally according the relation, In order to guarantee the stability of rotor up to 200Hz, five H∞ controllers are designed to compensate the gyroscopic effect, the stability and effectiveness are verified by the simulation.

II. THE MAGNETIC BEARING FLYWHEEL SYSTEM AND FEM MODEL

Figure.1 shows a magnetic bearing with a flywheel rotor which is about 13kg in weight and 0.65 meter in height and 0.6 meter in diameter. Fig.1(a) shows a flywheel with black CFRP part. Fig.1(b) is an assembly figure that RaAMB and AxAMB are electromagnet which is located in the direction of axial and radial. The gap of magnetic bearing and rotor is about 250 μ m.

To derive a flexible model, the rotor is considered as eight elements using the finite element method.[3] The flywheel was regarded as a concentration mass like Fig.2. Here, the mass of Element No.8 is regard to make an average each part at the bottom of the rotor. The electromagnet is arranged between element 2, 3, 7, and 8. Moreover, the damping and imbalance are not to be considered. So the equation derived from FEM as follows

$$\widetilde{\mathbf{M}}\ddot{\boldsymbol{q}} + \widetilde{\mathbf{G}}\dot{\boldsymbol{q}} + \widetilde{\mathbf{K}}\boldsymbol{q} = \widetilde{\mathbf{T}}\boldsymbol{U} \qquad (1)$$

where, $\widetilde{\mathbf{M}}$ is mass matrix, $\widetilde{\mathbf{G}}$ is gyroscopic matrix, $\widetilde{\mathbf{K}}$ is stiffness matrix, $\widetilde{\mathbf{T}}$ is a matrix which shows the position of magnetic bearing. q is state vector. ($\widetilde{\mathbf{M}}$, $\widetilde{\mathbf{G}}$, $\widetilde{\mathbf{K}} \in R^{36\times36}$ $\widetilde{\mathbf{T}} \in R^{36\times4}$, $\boldsymbol{q} \in R^{36\times4}$)

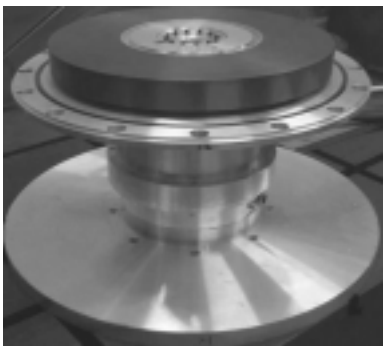

(a) Flywheel rotor and containment

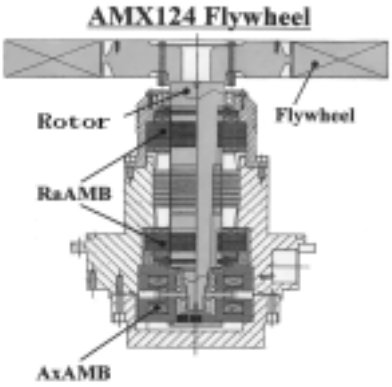

(b) Cross-sectional view

Fig.1 Overview of flywheel system

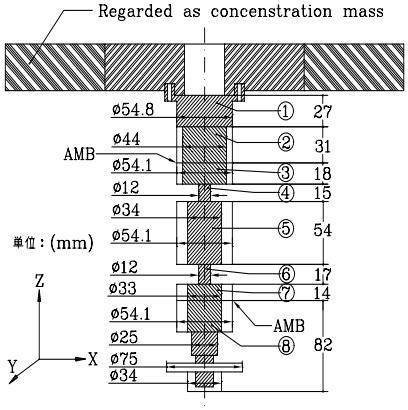

Fig.2 One dimensional finite element model

III. MODEL REDUCTION BASED ON SINGULAR DECOMPOSITION METHOD

A. cholsky decomposition

The order of FEM model are 72 as obtained from Eq.(1). It is necessary to reduce the orders of the model due to the limitation of computation speed of DSP. However, it is difficult to deal with a mode separation for obtaining a reduced-order model when a gyroscopic matrix exists in Eq.(1). So we adopt the method of L.Meirovitch to introducing a new state vector $\boldsymbol{z} = [\boldsymbol{q} \ \ \dot{\boldsymbol{q}}]^{\mathrm{t}}$. The form of equation will be as follow.

$$\mathbf{M}^* \dot{z}(t) + \mathbf{G}^* z(t) = \mathbf{T}^* \boldsymbol{U} \tag{2}$$

where,

$$\mathbf{M}^* = \begin{bmatrix} \widetilde{\mathbf{K}} & \mathbf{0} \\ \mathbf{0} & \widetilde{\mathbf{M}} \end{bmatrix} \quad \mathbf{G}^* = \begin{bmatrix} \mathbf{0} & -\widetilde{\mathbf{K}} \\ \widetilde{\mathbf{K}} & \widetilde{\mathbf{G}} \end{bmatrix} \quad \mathbf{T}^* = \begin{bmatrix} \mathbf{0} \\ \widetilde{\mathbf{T}} \end{bmatrix}$$

From Eq(2), We can obtain eigenvalue problem in standard form such as

$$s\mathbf{M}^* z(s) + \mathbf{G}^* z(s) = 0 \tag{3}$$

It is well known that the eigenvalues of Eq.(3) consist of n pairs of pure imaginary complex conjugates, $s_{\mathrm{r}} = \mathrm{i}\omega_{\mathrm{r}}$, $\bar{s}_{\mathrm{r}} = -\mathrm{i}\omega_{\mathrm{r}}$. Correspondingly, the eigenvectors also incur in pairs of complex conjugates, $z_{\mathrm{r}} = \boldsymbol{\alpha}_{\mathrm{r}} + i\boldsymbol{\beta}_{\mathrm{r}}$, . $\bar{z}_{\mathrm{r}} = \boldsymbol{\alpha}_{\mathrm{r}} - i\boldsymbol{\beta}_{\mathrm{r}} (\mathrm{r} \in 1 \cdots \mathrm{n})$ Where $\boldsymbol{\alpha}_{\mathrm{r}}$ is the real part and $\boldsymbol{\beta}_{\mathrm{r}}$ is the imaginary part of the eigenvector z_{r}. $\widetilde{\mathbf{G}}$ is still a skew matrix from the characteristic of K and G. Next, to introduce $s_{\mathrm{r}} = i\omega_{\mathrm{r}}$ and $z_{\mathrm{r}} = \boldsymbol{\alpha}_{\mathrm{r}} + i\boldsymbol{\beta}_{\mathrm{r}}$ into Eq.(2) and separate real part and imaginary part, we can acquire two forms of eigenvalue problem which is only related to x or y, such as

$$\begin{cases} \mathbf{K}^* \boldsymbol{\alpha}_{\mathrm{r}} = \lambda_{\mathrm{r}} \mathbf{M}^* \boldsymbol{\alpha}_{\mathrm{r}} \quad \mathbf{K}^* \boldsymbol{\beta}_{\mathrm{r}} = \lambda_{\mathrm{r}} \mathbf{M}^* \boldsymbol{\beta}_{\mathrm{r}} \\ \mathbf{K}^* = \mathbf{G}^{*\mathrm{T}} \mathbf{M}^{*-1} \mathbf{G}^* \quad \lambda_{\mathrm{r}} = \omega_{\mathrm{r}}^2 \end{cases} \tag{4}$$

Here, $\mathbf{K}^*$ has been a symmetric positive definite matrix. We can obtain n pairs repeated eigenvalures λ_{r}. Further, n pairs of 2n-dimensional eigenvectors $\boldsymbol{\alpha}_{\mathrm{r}}$ and $\boldsymbol{\beta}_{\mathrm{r}}$ are correspond to same λ_{r}. Here, to decompose $\mathbf{M}^*$, the cholsky decomposition is used like Eq(5). $\mathbf{Q}$ is upper three-corner procession.

$$\mathbf{M}^* = \mathbf{Q}\mathbf{Q}^{\mathrm{T}} \tag{5}$$

As we know, the condition for using the cholsky decomposition is that $\mathbf{M}^*$ must be positive definite and symmetric matrix. However, $\mathbf{M}^*$ become a semi-positive definite matrix in magnetic bearing system, when the rotor is in a "free-free" condition. Thus it is evident that the Cholsky decomposition is not suitable.

B Model Reduction by Singular Decomposition Method

For any matrix whose rank is r can be decomposed by the singular decomposition method such as Eq(6). Here, $\mathbf{U}$ and $\mathbf{V}$ are composed by the row vectors which are orthonormal vector.

$$\underset{\mathbf{n}\times\mathbf{m}}{\mathbf{M}^*} = \underset{\mathbf{n}\times\mathbf{r}}{\mathbf{U}} \ \underset{\mathbf{r}\times\mathbf{r}}{\mathbf{D}\,\lambda} \ \underset{\mathbf{r}\times\mathbf{m}}{\mathbf{V}^{\mathbf{T}}} \tag{6}$$

From the definition of the singular value decomposition method, it is obvious that $\mathbf{M}^*$ is not limited by the condition of positive definite. Therefore, we propose to use the singular decomposition method instead of cholsky decomposition method. Meanwhile, the row vectors of $\mathbf{U}$ are eigenvectors of $\mathbf{M}^*\mathbf{M}^{*\mathrm{T}}$ and the row vectors of $\mathbf{V}$ are eigenvectors of $\mathbf{M}^{*\mathrm{T}}\mathbf{M}^*$, Further, existence of an equation

of $\mathbf{M}^{*\mathrm{T}}\mathbf{M}^{*} = \mathbf{M}^{*}\mathbf{M}^{*\mathrm{T}}$ due to a real symmetric matrix $\mathbf{M}^{*}$, it is obvious that **U** has the same row vectors as **V** has. According to the above fact, we assume $\mathbf{R} = \mathbf{U}\sqrt{\mathbf{D}}$, so, the equation can be obtained as follow.

$$\begin{cases} \mathbf{R}^{\mathrm{T}} = \sqrt{\mathbf{D}}\mathbf{U}^{\mathrm{T}} = \sqrt{\mathbf{D}}\mathbf{V}^{\mathrm{T}} \\ \mathbf{M}^{*} = \mathbf{U}\mathbf{D}\mathbf{V}^{\mathrm{T}} = \mathbf{U}\sqrt{\mathbf{D}}\sqrt{\mathbf{D}}\mathbf{V}^{\mathrm{T}} = \mathbf{R}\mathbf{R}^{\mathrm{T}} \end{cases} \tag{7}$$

Although the form of Eq(7) is similar to Eq(5) of cholsky decomposition, it is different because **R** is not a upper three-corner procession. Introducing the equation into Eq(4), we can acquire a new equation s as follow.

$$\begin{cases} \boldsymbol{\varphi}\boldsymbol{P}_{\mathrm{r}} = \lambda_{\mathrm{r}}\boldsymbol{P}_{\mathrm{r}} \\ \boldsymbol{\varphi} = \mathbf{R}^{-1}\mathbf{K}^{*}\mathbf{R}^{-\mathrm{T}} \end{cases} \tag{8}$$

the eigenvector $\boldsymbol{P}_{\mathrm{r}} = [\boldsymbol{\alpha}_{\mathrm{r}} \quad \boldsymbol{\beta}_{\mathrm{r}}]$,(r=1,2,....,n) is response to eigenvalue λ_{r} Let us consider the line coordinates transformation $\boldsymbol{z}_{\mathrm{r}} = \mathbf{R}^{-\mathrm{T}}\boldsymbol{P}_{\mathrm{r}}\boldsymbol{\xi}$ and introducing it into Eq(2) , we can get a new equation as follow.

$$\dot{\boldsymbol{\xi}} = \boldsymbol{\theta}\boldsymbol{\xi} + \boldsymbol{\psi}\boldsymbol{f} \tag{9}$$

where

$$\boldsymbol{\theta} = -\mathbf{P}^{-1}\boldsymbol{\Lambda}\mathbf{P}, \quad \boldsymbol{\Lambda} = \mathbf{R}^{-1}\mathbf{G}^{*}\mathbf{R}^{-\mathrm{T}}, \boldsymbol{\psi} = \mathbf{P}^{-1}\mathbf{R}^{-1}\mathbf{T}^{*}$$

Here, $\boldsymbol{\xi} = [\boldsymbol{\eta}_{\mathrm{r}} \quad \boldsymbol{\zeta}_{\mathrm{r}}]$ is a mode coordinate and $\boldsymbol{\theta}$ is a block-diagonal matrix. Eq(9) is expressed in detail such as

$$\frac{\mathrm{d}}{\mathrm{dt}}\begin{pmatrix} \boldsymbol{\eta}_{1} \\ \cdots \\ \boldsymbol{\eta}_{\mathrm{n}} \\ - \\ \boldsymbol{\varsigma}_{1} \\ \cdots \\ \boldsymbol{\varsigma}_{\mathrm{n}} \end{pmatrix} = -\left(\begin{array}{ccc|ccc} 0 & 0 & 0 & \omega_{1} & 0 & 0 \\ 0 & \cdots & 0 & 0 & \cdots & 0 \\ 0 & 0 & 0 & 0 & 0 & \omega_{\mathrm{n}} \\ - & - & - & - & - & - \\ -\omega_{1} & 0 & 0 & 0 & 0 & 0 \\ 0 & \cdots & 0 & 0 & \cdots & 0 \\ 0 & 0 & -\omega_{\mathrm{n}} & 0 & 0 & 0 \end{array}\right)\begin{pmatrix} \boldsymbol{\eta}_{1} \\ \cdots \\ \boldsymbol{\eta}_{\mathrm{n}} \\ \cdots \\ \boldsymbol{\varsigma}_{1} \\ \cdots \\ \boldsymbol{\varsigma}_{\mathrm{n}} \end{pmatrix} + \mathbf{P}^{-1}\mathbf{R}^{-1}\mathbf{T}^{*}\boldsymbol{f} \tag{10}$$

C. reduced-order model

In this magnetic bearing flywheel system, the operational rotor speed is 12000 rpm, however, when the rotor approaches 6000 rpm, synchronous vibration of the first bending backward mode is regarded as a main cause which influences the system stability. So the reduced-order model including only rigid modes and the first bending backward mode are considered based on Eq(9) such as below.

$$\begin{cases} \dot{\boldsymbol{x}}_{\mathrm{r}} = \mathbf{A}_{\mathrm{r}}\boldsymbol{x}_{\mathrm{r}} + \mathbf{B}_{\mathrm{r}}\boldsymbol{U} \\ \boldsymbol{y}_{\mathrm{r}} = \mathbf{C}_{\mathrm{r}}\boldsymbol{x}_{\mathrm{r}} + \mathbf{D}_{\mathrm{r}}\boldsymbol{U} \end{cases} \tag{11}$$

where, $\mathbf{A}_{\mathrm{r}} \in \mathrm{R}^{10\times10}, \mathbf{B}_{\mathrm{r}} \in \mathrm{R}^{10\times4}, \mathbf{C}_{\mathrm{r}} \in \mathrm{R}^{4\times10}, \mathbf{D}_{\mathrm{r}} \in \mathrm{R}^{4\times4}$. The bode plots of actual system (FEM model) represented by a solid line and the reduced-order model by a dotted line shown in Fig.3. It is clear that eigen values in terms of the rigid mode are zero like Fig.3(a) while the rotor is in free-free condition. Fig.3(b) shows that both rigid mode and bending mode will be separated by a backward mode and forward mode while the coefficient spring is set and rotor is in rotation. The effectiveness of singular value decomposition can be verified through the result of mode separation.

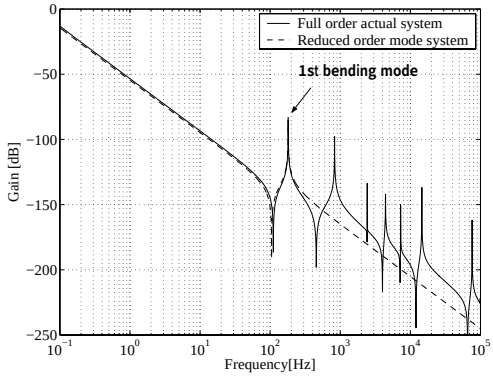

(a) Bode plot of free-free rigid-flexible rotor (0Hz)

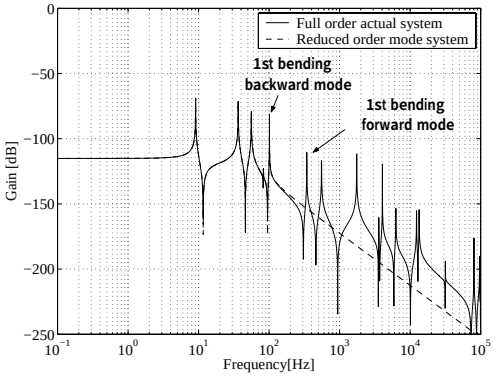

(b) Bode plot of rigid-flexible rotor (100Hz)

Fig.3 Mode separation

IV. VERIFICATION OF REDUCED-ORDER MODEL BY VIBRATION ANALYSIS

According to the characteristics that the natural frequencies of bending mode will keep its invariant, namely, the bending modes do not depend on controllers. So we can verify the reliability of reduced-order model based on the relation between natural frequency and rotational frequency. To obtain the relation, we did the vibration analysis based on the rigid model. Here, a controller designed based on rigid model which can keeps the system stable is used to obtain the natural frequency of closed-loop system. Firstly, a sinusoidal signal as a reference is inserted into the system to get the frequency response while the rotor is in levitation. The coherence of the input and output data is shown in Fig.4(a). Because the value of the coherence is almost one in all frequency range, it seems that the reliability of data is high. it is seems that the reliability of data is high. Further, the bode plot of the transfer function of the closed loop system is shown in Fig.4(b), where the rigid modes and the fist bending mode can be identified clearly.

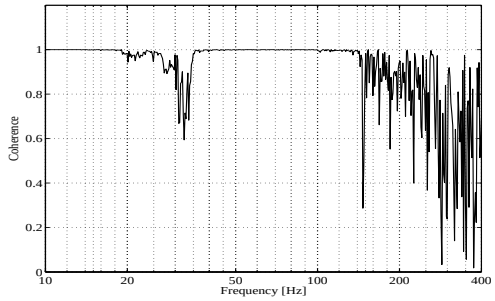

(a) Coherence

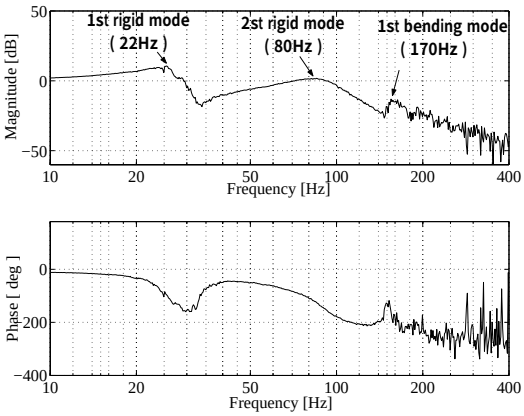

(b) Bode plot

Fig.4 Dynamic response at ω = 0Hz

Next, we inserted a sinusoidal signal into the system as reference while the rotor is in rotation and its speed is increases by 10Hz. Each gain plot of frequency response is shown in Fig.5. Figure5.(a) shows the first rigid mode which had been separated into a forward mode and a backward mode apparently. On the other hand, the variation of the second rigid mode and the first bending mode can not be distinguished easily because of not sharp peaks at 20Hz. When the rotational speed of the rotor is more than 30Hz, the first bending backward mode can also be distinguished , but the behaviour of the second rigid mode are not appeared without the resonance peak which corresponds to the synchronous frequency of the rotor like (b),(c),(d). From these result; especially (d) where the first bending backward mode had approached 112Hz, thus the reason of the rotor touchdown near 110Hz is quite evident Figure.6 gives a summary of behaviour of the natural frequency based on the data of vibration analysis, where the simulation result is shown too. The sign ○ represents the experiment value and dotted line represents a calculation value. We can draw a conclusion that the reliability of the derived flexible model is high according to the variation of the first bending mode whose calculated value match the experiment value well.

.

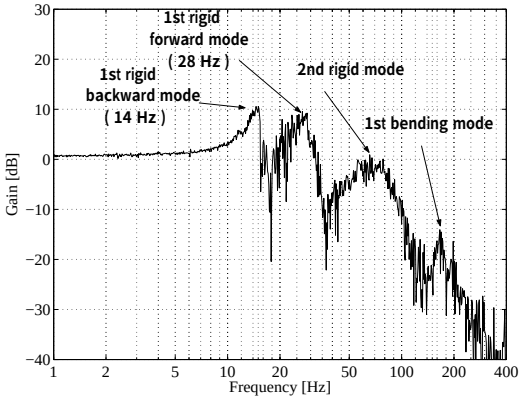

(a) Bode plot at ω =20Hz

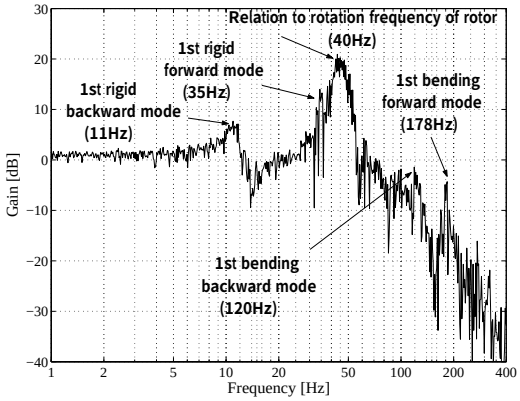

(b) Bode plot at ω =40H

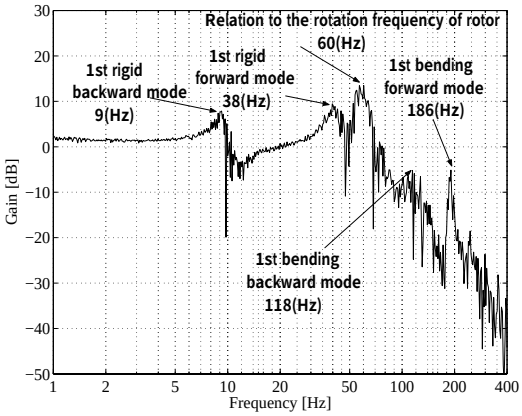

(c) Bode plot at ω =60Hz

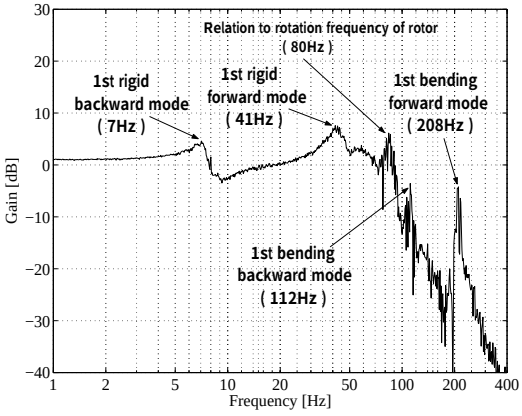

(d) Bode plot at ω =80Hz

Fig.5 Dynamic response in rotation

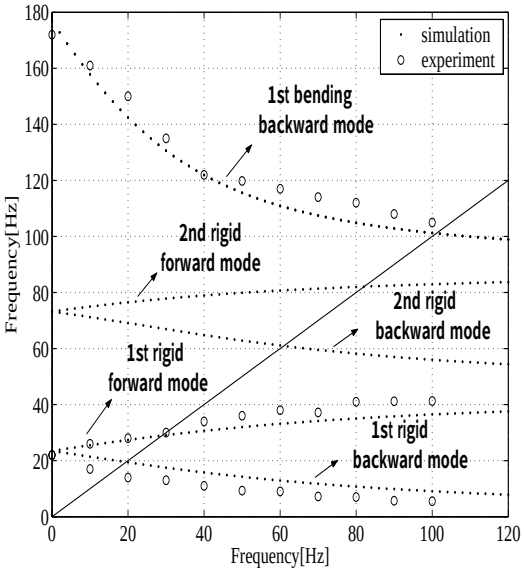

Fig.6 Relation bewteen natrual frequency and rotational frequency

V. THE DESINGN OF H_∞ CONTROLLER

In the magnetic bearing system, it is necessary to design a servo system. Further, to avoid the unstable influence brought by disregarded higher-order bending mode, the stabilization of robustness about spillover problem become important too. Thus, we use the H_∞ control theory to design a controller which can satisfy such demands. The Block diagram of generalized plant is shown in Fig.7. Firstly, a H_∞ control without considering gyroscopic effect is designed while the rotor is in levitation. The weighting functions are such as Eq.(12). W_s is designed as the 1st order filter and W_t as the 2nd order filter and its bode plot shown in Fig.8(a).

$$Ws = 10^{-3} \times \frac{s+10}{s+0.01}$$
$$Wt = 10^{-5} \times \left(\frac{s+3000}{s+400000}\right)^2 \qquad (12)$$

Fig.8(b) shows the bode plot of the H_∞ controller. It is understood that the controller is a servo controller which has a strong rigidity for disturbance in the low frequency range. Fig.8(c) shows the bode plot of open and closed-loop system applied the designed H_∞ controller to actual system, the gain plot of the closed-loop system represented by a dotted line and open system without controller by a solid line.

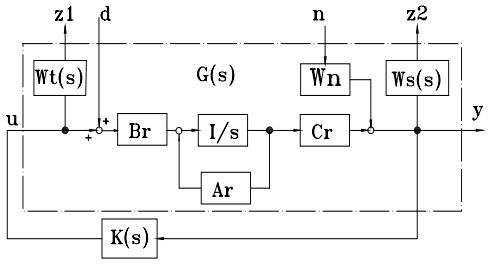

Fig.7 Block diagram of generalized plant

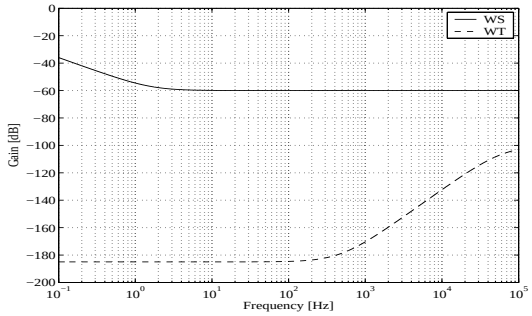

(a) Bode plot of weighting function

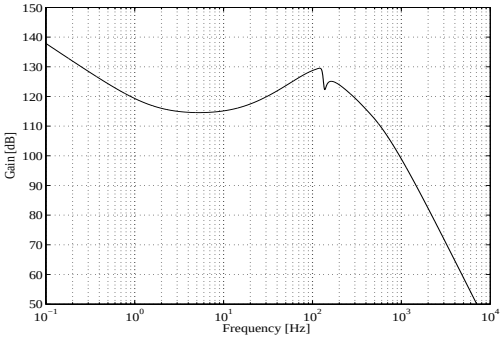

(a) Bode plot of H_∞ servo controller

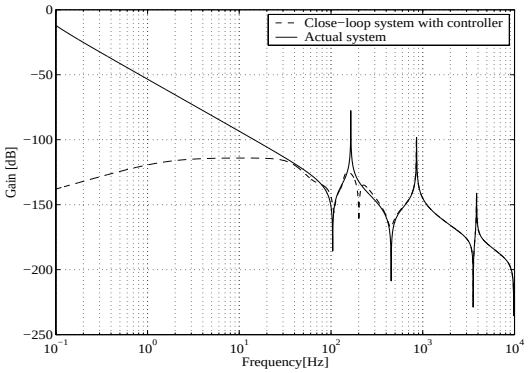

b Bode plot of open and close-loop system

Fig.8 Bode plot of 0Hz

On the other hand, the controller designed in levitation was applied to high rotation speed like 5Hz or more, the system will become unstable due to the gyroscopic effect that is generated in rotation. Some eigenvalues of closed-loop system will move to the right side of complex plane. To solve this problem ,We designed four H_∞controllers again during all rotation range. Each controller is designed based on the model set the rotation speed as 50Hz, 100Hz, 150Hz, or 200Hz. Fig.9 (a) shows the comparison result of the gain plots of four controllers where two peaks of gain exist. Because both the peak I in Fig.9 (a) and the first rigid backward mode in Fig.6 is moving to the lower frequency in common following the increase of rotation frequency, We can draw a conclusion that the peak I is mainly to control the first rigid backward mode. As the

same reason that the second peak II is mainly to control the first bending backward mode. Namely, the two modes have a larger influence on the stability of the system. Meanwhile, the high gain is necessary to be provided for the system stabilization. Fig.9(b) shows the gain plot of closed-loop system using the controller designed at 150Hz to be applied the FEM model set ω=100Hz. It is obvious that the designed controller has a robustness to compensate the gyroscopic effect because all of poles lie in left complex plane like Fig.9(c). Finally, we can draw a conclusion that the stability of system can be guaranteed by switching the five H_∞ controllers in rotation range from 0 to 200Hz.

CONCLUSION

Magnetic bearing system is an extremely unstable system by nature, therefore, it is important to design a controller based on an accurate mode. The FEM model with gyroscopic effect was derived in the flywheel magnetic bearing system and a reduced-order modal is obtained by the singular value decomposition, the conclusion about the effectiveness of modal and controller is such as following.

(1) The singular value decomposition is proposed instead of Cholsky decomposition, and the effectiveness was verified

(2).The reliability of the FEM flexible model is verified based on the relationship between natural frequency and rotation frequency by vibration analysis.

(3) The rotor is controlled by five H_∞ controllers which are scheduled by rotation speed in the range from 0Hz to 200Hz. Each controller can stabilize the rotor in the range of 50Hz.

(4) The first rigid backward mode and bending backward mode cause serious influence on system stability which can be seen from the two peaks existing in the gain plot of H_∞ controllers

REFERENCES

[1] M.ren, K.nonami,, Zero Bias Backstepping Control of Magnetic Bearing System with Gyroscopic Effec (Consideration based on rigid model and flexible model, Trans.Japan Society of Mechanical Engineers (C), Vol.71,No.712, 2005, pp.3437-3444

[2] L.Meirovitch,Computational Methods in Structural Dynamics, Sijthoff Noordhoff international Publishers B.V., 1980

[3] K.Nonami, Response in Passing Through Critical Speed for Arbitrary Distributed Flexible Rotor Systems (Part1), Trans.Japan Society of Mechanical Engineers(c), Vol.48, No.435, 1982, pp.1669-1677

[4] Y.J.Zhang, K.Nonami, H.Higasa, Zero Power Control of 10MWh Class Energy Storage Flywheel System Using Superconducting Magnetic Bearing with Gyroscopic Effect, JSAEM , Vol.10, No.2, 2002, pp.208-216

[5] S. Sivrioglu, K. Nonami, Active Permanent Magnet Support for a Superconducting Magnetic Bearing Flywheel Rotor, IEEE Transactions on Applied Superconductivity, vol.10, no.4, 2000, pp.1673-1677

[6] S. Sivrioglu, K. Nonami, M. Saigo, Low Power Consumption Nonlinear Control with H-infinity Compensator for a Zero-Bias Flywheel AMB System,Journal of Vibration and Control, vol.10, no. 8, pp.1151-1166, 2004.

[7] T.A.Coombs, Superconducting Magnetic Bearings for Energy Storage Flywheels, IEEE Tran. on Applied Superconductivity, Vol.9, No.2 June, 1999, pp.968-991

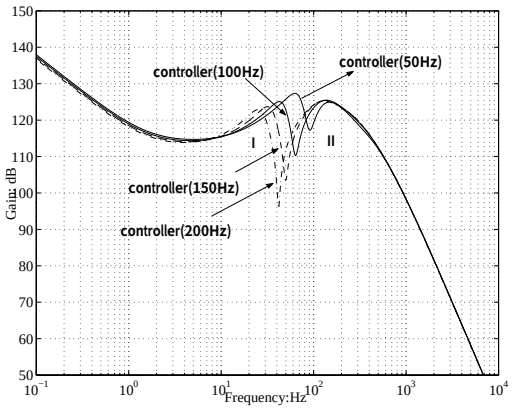

(a) Bode plot of four H_∞ controller

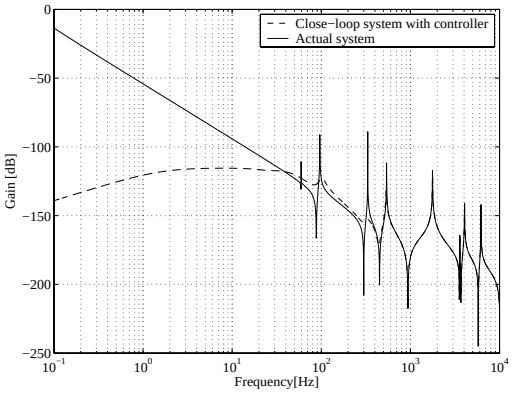

(b) Bode plot of open and closed-loop system at 100Hz

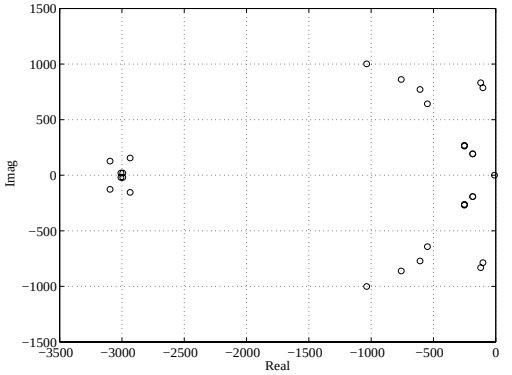

(c) Poles of closed- loop system at 100Hz

Fig.10 Result of stability at 100Hz with controller at 150Hz

[8] S.Okamoto, M.Sakata, K.Kimura, H.Ohnabe, Finite Element Vibration Analysis of a Flexible Rotor Subjected to Base Excitation (2nd Report, Flexible Suspension-Flexible Shaft-Flexible Disk-Flexible Blade System), Trans.Japan Society of Mechanical Engineers (C), Vol.58, No.549, 1992, pp.1352-1359

[9] H.Kameno et al, Basic Design of 1kWh Class Flywheel Energy Storage System, Proceedings of The Eighth International Symposium on Magnetic Bearings (ISMB-8) , pp.575-580, 2002

[10] A.Kubo et al, Dynamic Analysis and Levitation Test in 1kWh Class Flywheel Energy Storage System, Proceeding of 7th International Symposium on Magnetic Technology (ISMST-7), pp.144-149,2003